Crystal Structure of an Actinidin–E-64 Complex[†,‡]

Kottayil I. Varughese,[*,§,∥] Ying Su,[⊥] Dean Cromwell,[§] Sadiq Hasnain,[▽] and Nguyen-huu Xuong[§,⊥,#]

Departments of Biology, Chemistry, and Physics, University of California at San Diego, La Jolla, California 92093-0317, Department of Molecular and Experimental Medicine, The Scripps Research Institute, 10666 North Torrey Pines Road, La Jolla, California 92037, and Institute for Biological Science, National Research Council of Canada, Ottawa, Ontario K1A 0R6, Canada

Received October 2, 1991; Revised Manuscript Received February 10, 1992

ABSTRACT: E-64, 1-(L-*trans*-epoxysuccinylleucylamino)-4-guanidinobutane, is a potent and highly selective irreversible inhibitor of cysteine proteases. The crystal structure of a complex of actinidin and E-64 has been determined at 1.86-Å resolution by using the difference Fourier method and refined to an *R*-factor of 14.5%. The electron density map clearly shows that the C2 atom of the E-64 epoxide ring is covalently bonded to the S atom of the active-site cysteine 25. The charged carboxyl group of E-64 forms four H-bonds with the protein and thus may play an important role in favorably positioning the inhibitor molecule for nucleophilic attack by the active-site thiolate anion. The interaction features between E-64 and actinidin are very similar to those seen in the papain–E-64 complex; however, the amino-4-guanidinobutane group orients differently. The crystals of the actinidin–E-64 complex diffracted much better than the papain–E-64 complex, and consequently the present study provides more precise geometrical information on the binding of the inhibitor. Moreover, this study provides yet another confirmation that the binding of E-64 is at the S subsites and not at the S′ subsites as has been previously proposed. The original actinidin structure has been revised using the new cDNA sequence information.

E-64, 1-(L-*trans*-epoxysuccinylleucylamino)-4-guanidinobutane (**1**; Chart I), is a potent and irreversible inhibitor of many cysteine proteases, such as actinidin, papain, ficin, and cathepsins B and L (Rich, 1986). This inhibitor was isolated as a natural product from cultures of *Aspergillus japonicus* (Hanada et al., 1978a), and its chemical structure was determined by Hanada et al. (1978b). The E-64 molecule consists of three components, epoxysuccinyl, leucyl, and amino-4-guanidinobutane, and its terminal carboxyl and guanidinium groups are negatively and positively charged, respectively, at neutral pH.

Potent cysteine protease inhibitors can serve not only as useful tools in the study of cysteine proteases but also as potential therapeutic drugs for diseases caused by abnormal elevation of proteolytic activity (Kar & Pearson, 1976; Sugita, 1988). A knowledge of the inhibitory mechanism of E-64 could be valuable for the design of more potent and specific cysteine protease inhibitors leading to clinically useful drugs.

The crystal structure of a papain–E-64 complex has been recently determined by Varughese et al. (1989). Here we report the crystal structure of an actinidin–E-64 complex. The crystal structure of actinidin, a cysteine protease isolated from the fruit of *Actinidia chinensis*, has been determined at 1.7-Å resolution by Baker (1980). The tertiary structures of actinidin and papain share a remarkable similarity, and their polypeptide backbones are virtually superimposable although their primary sequences are only 48% identical (Kamphuis et al., 1985). The structure of the actinidin–E-64 complex described below shows that the binding of E-64 to actinidin is very similar to that seen in the papain–E-64 complex. The complex is formed through a covalent linkage between the γ sulfur of the active-site cysteine 25 and the C2 atom of the inhibitor.

Chart I: Structure of E-64 (**1**)

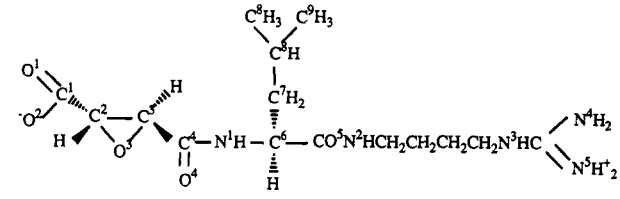

Experimental Procedures

Actinidin was purified according to the procedure of Brocklehurst et al. (1981). The purified enzyme was precipitated by adding $(NH_4)_2SO_4$ to 50% saturation and stored until required. To make the actinidin–E-64 complex, 1 mL of actinidin (about 8 mg/mL) suspension was activated by adding 3 mL of solution containing 200 mM Tris-HCl and 40 mM cysteine at pH 8.0. After incubation for 15 min at 22 °C, 0.6 mg of DTT was added to the solution. The solution was then passed through a G15 Sephadex column, and the peak fractions were collected. The collected fractions were mixed with 0.2 mg of E-64, and the solution was then concentrated using a colloidin bag to a concentration of 5 mg/mL, which was used for crystallization.

The crystals were grown by the hanging drop method at 4 °C. The drops contained 5 μL of the protein solution and 5 μL of the reservoir solution which had 1.4 M $(NH_4)_2SO_4$, 2.5 mM $Na_2S_4O_6$, and 20 mM MES with a pH of 6.0. The crystals were orthorhombic, $P2_12_12_1$, a = 78.47 Å, b = 81.81

[†] This investigation was supported in part by Grants RR0144 (UCSD) from NIH and DIR88-22385 from NSF (UCSD) and by Lucille P. Marky Foundation (UCSD).

[‡] The atomic coordinates for the crystal structure in this paper have been deposited with Brookhaven Protein Data Bank, under the filename 1AEC.

[*] To whom correspondence should be addressed.

[§] Department of Biology, University of California at San Diego.

[∥] Department of Molecular and Experimental Medicine, The Scripps Research Institute.

[⊥] Department of Chemistry, University of California at San Diego.

[▽] Institute for Biological Science, National Research Council of Canada.

[#] Department of Physics, University of California at San Diego.

0006-2960/92/0431-5172$03.00/0

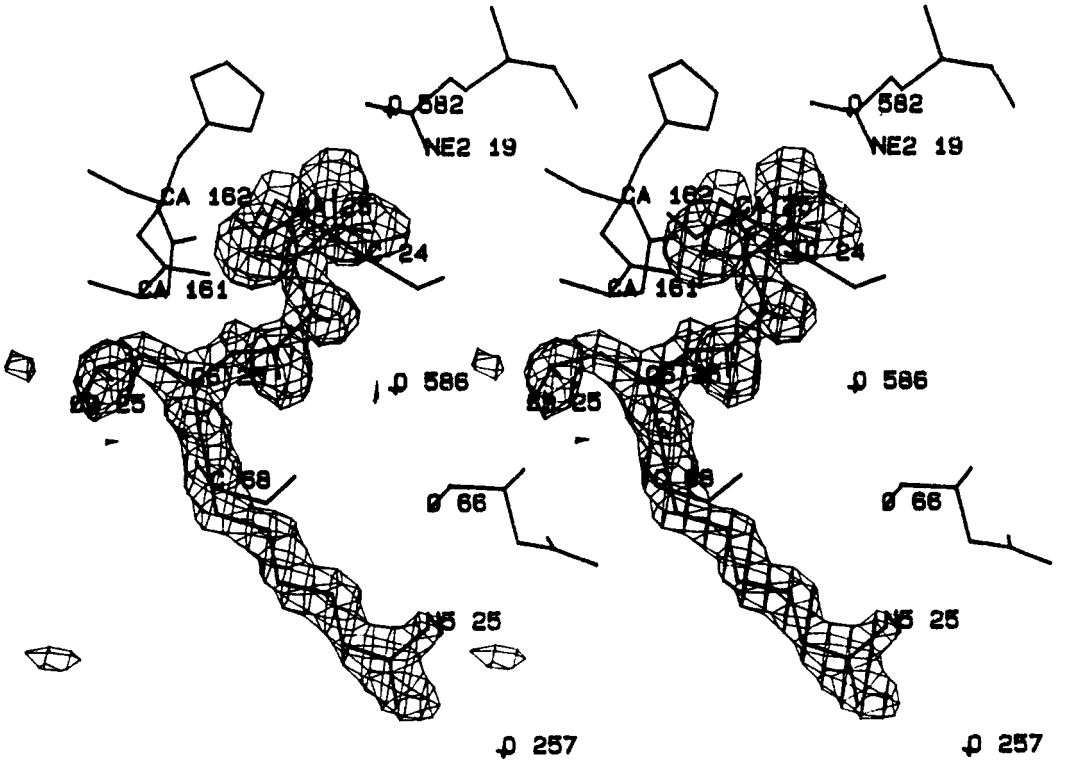

FIGURE 1: Stereoview of an omit map showing the electron density of E-64.

Å, c = 32.93 Å. The native protein crystals belonged to the same space group, a = 78.2 Å, b = 81.9 Å, c = 33.02 Å (Baker, 1980).

The diffraction data were collected using the Xuong-Hamlin multiwire system at the University of California, San Diego (Xuong et al., 1985). A total of 20 orientations were collected at 4 °C. The statistics on the data collection are the following: number of observations, 96911; number of unique reflections, 17408; and the average $I/\sigma(I)$ of 4.6 at a resolution of 1.86 Å. The data is complete to 98% at 2.0 Å and 94% at 1.86 Å.

Electron Density Maps and Refinement

Twenty cycles of conventional refinement with the program package X-PLOR (Brunger et al., 1987) were carried out using the coordinates of the native structure along with the water molecules, but leaving out the S atom of the cysteine 25. This refinement gave an R-factor of 25.7%. A $(F_o - F_c)$ electron density map was computed at this stage, which clearly showed the density of the S atom and the inhibitor moiety (Figure 1). The model for the inhibitor was fitted into the $(F_o - F_c)$ map by using the program FRODO (Jones, 1975) on a Silicon Graphics IRIS 4D work station. The refinements were carried out on the San Diego Super Computer CRAY 4-MP8/864. Sixty cycles of conventional refinement using crystallographic data between 8-Å and 2.0-Å resolution resulted in a decrease in the R-factor from 25.7% to 18.5%. Thirteen water molecules were excluded from the refinement because of their close contacts with the inhibitor. Another 40 cycles of temperature factor refinement dropped the R-factor to 15.9%. At this stage, an $(F_o - F_c)$ map was computed without the inhibitor and the terminal guanidinium group was refitted. The difference electron density map also revealed an additional 8 water molecules which were different from the excluded water molecules. The newly reported protein sequence of actinidin, deduced from its cDNA sequence, has 17 corrections (Prodivinsky et al., 1989) from the sequence used by Baker (1980). Therefore, several omit maps were calculated in order to correct these residues. For residues 41, 66, 80, 99, 104, and 105, the old and new assignments fit equally well in the electron density map because the only change is that one oxygen is corrected to a N atom. Even though electron density cannot distinguish between the new and old assignments in these cases, the residue assignments were done according to the new sequence (Prodivinsky et al., 1989). The sequence corrections are listed in Table I. The maps clearly support the corrections on residues 42, 44, 148, 160, 165, 164, and 175, and two typical examples are shown in Figure 2. (Residues 42 and 44 were treated as disordered in the native crystal structure.) Density for residue 100 shows that it is a Val instead of a Leu. Density for residue 101 does not show the oxygens of Asp. We took it as an Ala for the refinement. Residue 146 has a very weak density for the side chain and does not support the sequence correction to His, and hence we assigned it as Gln for the refinement. Thus, for residues

Table I: Residue Correction in the Refinement

residue no.	old assignment[a]	new assignment[b]	electron density favors	assignment in the final refinement
41	Thr	Val	both	Val
42	Ser	Thr	Thr	Thr
44	Ser	Val	Val	Val
66	Asp	Asn	both	Asn
80	Asp	Asn	both	Asn
97	Asp	Glu	none	Glu
99	Asp	Asn	both	Asn
100	Val	Leu	Val	Val
101	Ala	Asp	Ala	Ala
104	Asp	Asn	both	Asn
105	Gln	Glu	both	Glu
146	Gln	His	none	Gln
148	Ala	Ser	Ser	Ser
160	Val	Ile	Ile	Ile
164	Ile	Val	Val	Val
165	Val	Thr	Thr	Thr
175	Val	Ile	Ile	Ile

[a] Baker (1980) and Craine and More (1978). [b] Podivinsky et al. (1989).

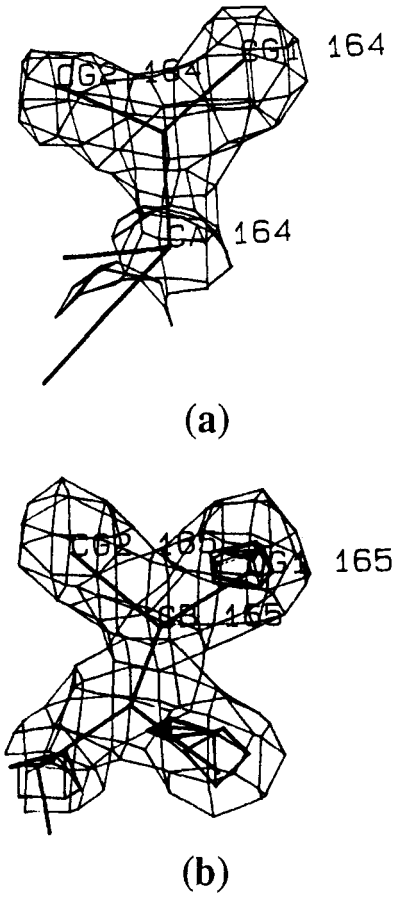

FIGURE 2: (a) Electron density in an omit map showing the density for residue 164. The density supports the sequence correction (Podivinsky et al., 1989) that it is Val and not Ile. (b) Density for residue 165. OG1 has larger density than CG2, supporting the sequence correction. Moreover, OG1 is involved in a hydrogen-bonding interaction with a water molecule.

100, 101, and 146, we retained the old sequence assignments. For residue 97, density beyond CB was poor; however, we assigned it as Glu. The disordered residues 9, 58, and 129 in the native structure were also checked on an omit map. The map shows that residue 9 is disordered but not residue 129. The side chain of Arg 58 was reoriented, and an additional water molecule was located in the vicinity which forms a H-bond with residue 58. Side chains of residues 8, 114, and 211 were examined and reoriented because of unusual density seen in the $(F_o - F_c)$ map. Residue 130 does not have density for the whole tyrosine ring. Only CG, CD1, and CE1 are seen. After the above corrections were made, 40 cycles of conventional refinement were performed using data with $I \geq 2\sigma(I)$ between 8 Å and 1.86 Å, and the final R-factor was 14.6%. Then, 30 cycles of temperature factor refinement were performed, and this yielded an R-factor of 14.5%. The number of reflections used in the refinement of the structure is 17 116 which is 98.3% of the total number of unique reflections measured. The rms deviations of bond distances and angles from ideality are 0.014 Å and 2.4°, respectively, in the final model. The atomic coordinates of the structure have been deposited with the Protein Data Bank, Chemistry Department, Brookhaven National Laboratory, Upton, NY 11973.

Results and Discussion

The complete E-64 molecule is well defined in the electron density map (Figure 1). The map clearly shows that the C2 atom of the E-64 epoxide ring is covalently bonded to the S atom of the active-site cysteine 25. The bond distance between C2 and S is 1.81 Å. The chirality of C2 changes from L-form in E-64 to D-form in the complex. Table II lists all of the H-bonds involving E-64 and the protein in the actinidin–E-64 and papain–E-64 (Varughese et al., 1989) complexes. The carboxylate of E-64 has a strong interaction with the active site of actinidin. One of the carboxylic oxygens (O2) forms three H-bonds with the protein, one to the side chain of glutamine 19 and the other two to the backbone NH of cysteine 25 and glycine 24, respectively. The other carboxylic oxygen (O1) also has two H-bonds, one to the imidazole ring ND1 of histidine 162 and another to a water molecule.

Table II: Hydrogen Bonding Interactions of E-64 with Actinidin and Papain

E-64	protein[a]	distance (Å)
O1	ND1(162), ND1(159)[b]	2.75
		2.90
O1	O(H_2O582), O(H_2O217)	2.73
		2.67
O2	NE2(19), NE2(19)	2.86
		2.87
O2	N(25), N(25)	2.89
		2.95
O2	N(24), N(24)	3.33
		3.11
O3	O(H_2O586)	2.65
O4	N(68), N(66)[b]	2.90
		2.88
N1	O(161), O(158)[b]	3.10
		3.40
N2	O(68), O(66)[b]	2.87
		3.04
N3	O(H_2O54)	2.97
N4	O(H_2O54), OH(61)	3.49
		2.96
N4	O(H_2O257), O(H_2O216)	3.43
		2.45
N5	O(66), OH(67)	3.35
		2.93

[a] The first value corresponds to the present study, and the second value corresponds to the papain–E-64 complex (Varughese et al., 1989). [b] Although these residue numbers are different, they are equivalent to those of actinidin in the sequence alignment.

Fluorescence studies showed that the pK_a of His 159 in the papain–E-64 complex is 7.0. We expect His 162 of actinidin to have a similar pK_a value when the enzyme is complexed with E-64 and ND1 to be protonated as the crystals were grown at pH 6.0. Therefore, ND1 must act as the donor in the ND1(162)···O1 interaction. O3 is hydrogen bonded to a water molecule with an O···O distance of 2.65 Å. The E-64 leucyl side chain occupies the entry to the hydrophobic pocket of actinidin's S_2 subsite (Figure 3). The interaction between glycine 68 and E-64 constitutes a one-residue stretch of parallel β-sheet. These interactions are also found to be the same in the papain–E-64 complex. Those similar interactions imply that the carboxyl group and the leucyl group play important roles in favorably positioning the E-64, facilitating the bond formation between E-64 and cysteine 25 of the protein. The importance of the role of the carboxylate was supported by the experimental result that esterification of the free carboxyl of the epoxysuccinyl group in E-64 or related analogues decreases the rate of inactivation (Rich, 1986). The amino-4-guanidinobutane group of E-64 has much less interaction with actinidin. This part of E-64 orients differently in the actinidin–E-64 and papain–E-64 complexes. This is consistent with the fact that the amino-4-guanidinobutane residue can be replaced with a variety of alkyl and amino groups without loss of activity (Rich, 1986). Figure 4 depicts a superposition of the active sites of the actinidin–E-64 complex and papain–E-64 complex. The main difference between the two is in the

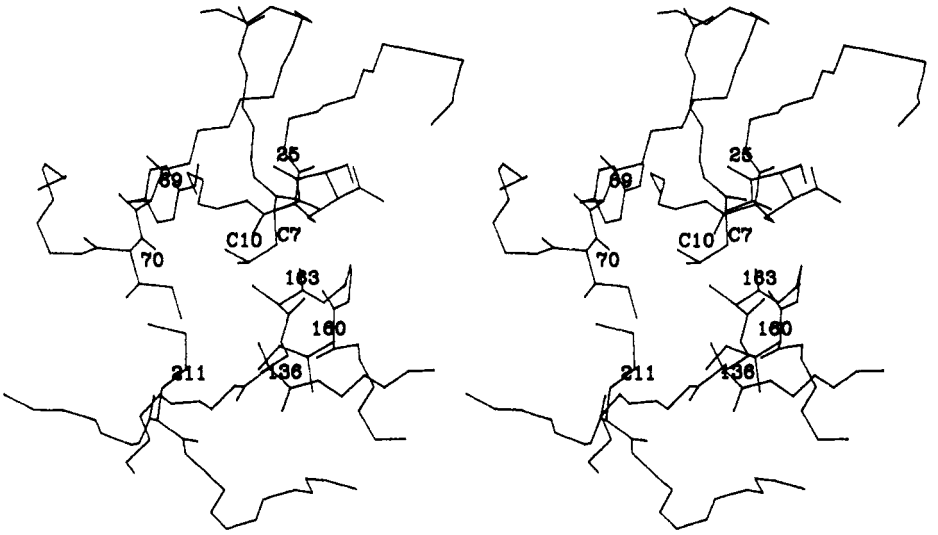

FIGURE 3: The leucyl group of E-64 is located in the hydrophobic pocket of the S2 subsite. Residues Tyr 69, Ile 70, Ala 136, Ile 160, and Met 211 form the hydrophobic pocket.

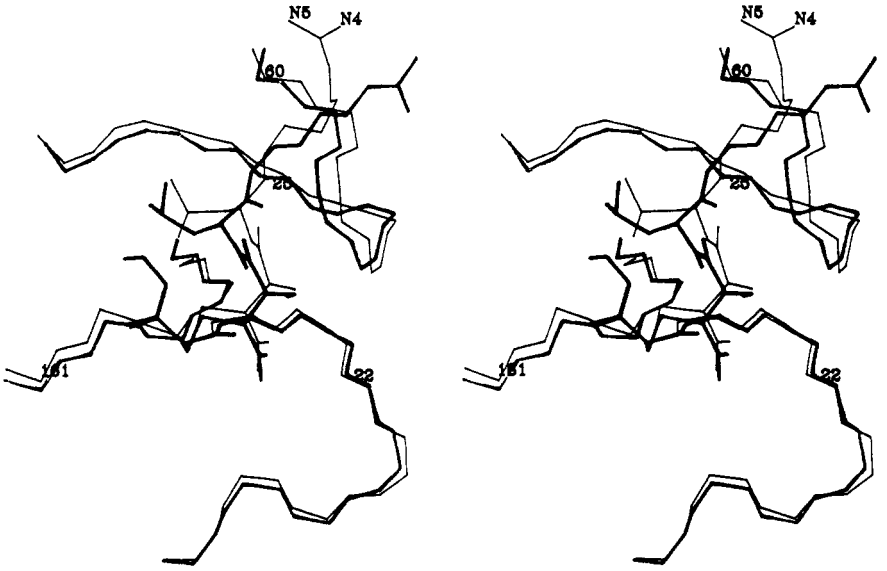

FIGURE 4: Superposition of the active sites of the actinidin–E-64 complex (thick line) and the papain–E-64 complex (thin line).

Scheme I: Attack of Thiolate Group on E-64[a]

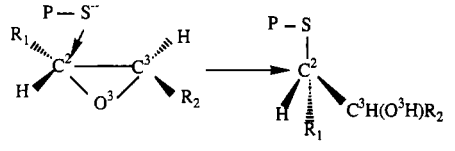

backside attack inversion of configuration at C2

[a] R_1 = $-CO_2-$; R_2 = $-CONHCH(CH_2CH(CH_3)_2)CONH-(CH_2)_4NCH(NH_2)_2^+$; P = actinidin–$Cys^{25}$–.

orientation of the amino-4-guanidinobutane group.

The attack of the active-site thiol group of cysteine proteases occurs from the backside of the E-64 and results in the opening of the epoxide ring and at the same time the formation of a covalent bond between the inhibitor and the enzyme (likely an S_N2 reaction). Consequently, the configuration of the C2 is inversed from the L-form to the D-form (Scheme I). It had been previously proposed (Rich, 1986; Barret et al., 1982) that the binding of E-64 is in the S′ subsites (Schechter & Berger, 1967). However, the present study and the study on the papain–E-64 complex (Varughese et al., 1989) and the papain–E-64-c complex (Yamamoto et al., 1990) confirm that the binding is at the S subsites (Schechter & Berger, 1967). This dependence on the unprimed subsites for stabilizing interaction energies is also evident in the X-ray crystal structure of the papain–stefin complex (Stubbs et al., 1990) and from the docking studies with the crystal structures of egg white cystatin and papain (Bode et al., 1988; Machleidt et al., 1989; Turk & Bode, 1991). The structures of the cystatin and stefin complexes with papain also show stabilizing interactions with Gln 19 of papain which has been shown to form part of the oxyanion hole (Menard et al., 1991). Apart from the larger size of the stefin (M_r about 11 000) and cystatin (M_r about 13 000) which enables a larger number of interactions with the enzyme, a major difference in the mode of interaction is that papain does not form a covalent complex with or cause the hydrolysis of the cystatin or stefin peptide backbone (Stubbs et al., 1990).

REFERENCES

Baker, E. N. (1980) *J. Mol. Biol. 141*, 441–484.

Barrett, A. J., Kembhavi, A. A., Brown, M. A., Kirschke, H., Knight, C. G., Tamai, M., & Hanada, K. (1982) *Biochem. J. 201*, 189–198.

Bode, W., Engh, R., Musil, D., Thiele, U., Huber, R., Karshikov, A., Brzin, J., Kos, J., & Turk, V. (1988) *EMBO J. 7*, 2593-2599.
Brocklehurst, K., Baines, B. S., & Malthouse, J. P. G. (1981) *Biochem. J. 197*, 739-746.
Brunger, A. T., Kuriyan, J., & Karplus, M. (1987) *Science 235*, 458-460.
Carne, A., & Moore, C. H. (1978) *Biochem. J. 173*, 73-83.
Hanada, K., Tamai, M., Yamagishi, S., Ohmura, S., Sawada, J., & Tanaka, I. (1978a) *Agric. Biol. Chem. 42*, 523-528.
Hanada, K., Tamai, M., Ohmura, S., Sawada, J., Seki, T., & Tanaka, I. (1978b) *Agric. Biol. Chem. 42*, 529-536.
Jones, T. A. (1975) *J. Appl. Crystallogr. 11*, 268-272.
Kamphuis, I. G., Drenth, J., & Baker, E. N. (1985) *J. Mol. Biol. 182*, 317-329.
Kar, N. C., & Pearson, C. M. (1976) *Clin. Chim. Acta 73*, 293-297.
Machleidt, W., Thiele, U., Laber, B., Assfalg-Machleidt, I., Esterl, A., Wiegand, G., Kos, J., Turk, V., & Bode, W. (1989) *FEBS Lett. 243*, 234-238.
Menard, R., Carriere, J., Laflamme, P., Plouffe, C., Khouri, H. E., Vernet, T., Tessier, D. C., Thomas, D. Y., & Storer, A. C. (1991) *Biochemistry 30*, 8924-8928.
Podivinsky, E., Forster, R. L. S., & Gardner, R. C. (1989) *Nucleic Acids Res. 17*, 8363-8363.
Rich, D. (1986) in *Proteinase Inhibitors* (Barrett & Salvesen, Eds.) pp 153-178, Elsevier, Amsterdam.
Schechter, I., & Berger, A. (1967) *Biochem. Biophys. Res. Commun. 27*, 157-162.
Stubbs, M. T., Laber, B., Bode, W., Huber, R., Jerala, R., Lenarcic, B., & Turk, V. (1990) *EMBO J. 9*, 1939-1947.
Sugita, H. (1988) *Medicina 22*, 282-295.
Turk, V., & Bode, W. (1991) *FEBS Lett. 285*, 213-219.
Varughese, K. I., Ahmed, F. R., Carey, P. R., Hasnain, S., Huber, C. P., & Storer, A. C. (1989) *Biochemistry 28*, 1330-1332.
Xuong, N. H., Sullivan, D., Neilson, C., & Hamlin, R. (1985) *Acta Crystallogr. B41*, 267-269.
Yamamoto, D., Ishida, T., & Inoue, M. (1990) *Biochem. Biophys. Res. Commun. 171*, 711-716.

Supplementation of the Phosphatidyl-L-serine Requirement of Protein Kinase C with Nonactivating Phospholipids†

Myung-Ho Lee and Robert M. Bell*
Department of Biochemistry, Duke University Medical Center, Durham, North Carolina 27710
Received June 10, 1991; Revised Manuscript Received March 13, 1992

ABSTRACT: The mechanism of protein kinase C (PKC) activation by phosphatidyl-L-serine (PS) is highly specific and occurs with high cooperativity [Lee, M.-H., & Bell, R. M. (1989) *J. Biol. Chem. 264*, 14797-14805]. To further investigate the multiplicity and specificity of PS cofactor requirement, some of the PS molecules present in Triton X-100 mixed micelles were substituted with nonactivating phospholipids devoid of required amino or carboxyl functional groups. The ability of these phospholipids to spare or reduce the mole percent of PS required was determined. Addition of phosphatidyl-(3-hydroxypropionate) (PP) or phosphatidate (PA) reduced the mole percent of PS required for maximal activity from 10 to 4 mol %, and also reduced the cooperativity of activation with PS. In contrast, phosphatidylethanolamine did not alter the dependence on PS. Phosphatidylethanol (P-Et) reduced the PS requirement to 2-4 mol % and cooperativity less efficiently than PP or PA. Phosphatidylglycerol and phosphatidylinositol resemble P-Et in their ability to reduce PS requirements and cooperativity. Therefore, it appears that the ability of phospholipids to substitute for PS in PKC activation depends on the negative charge in the phospholipid head group and the efficiency of substitution appears to be directly related to the negative charge density. The presence of two acyl groups within the phospholipid cofactor proved important since lyso-PS and lyso-PA replaced a portion of PS molecules required less efficiently than P-Et. Sodium oleate and sodium dodecyl sulfate behaved like lyso-PS. When other anionic lipids are present, approximately four molecules of PS per micelle are required for maximal PKC activity. These data indicated that there are two distinct sets of lipid-protein interactions occurring when PKC activation occurs. One set of interactions displays high specificity for PS. The other set of interactions is far less specific and involves anionic lipids. These data raise the possibility that acidic lipids, notably PA, may regulate PKC activity in cells.

Protein kinase C (PKC),[1] a Ca^{2+}-, DAG-, and phospholipid-dependent serine/threonine-specific protein kinase, has a crucial role in cellular signal transduction [for a review, see Nishizuka (1984a,b)]. When cells are activated by hormones and growth factors which generate DAG in the inner leaflet of the plasma membrane, or treated with tumor-promoting phorbol esters, PKC associates with the membrane and becomes active (Kikkawa et al., 1983; Kraft & Anderson, 1983; Fearon & Tashjian, 1985; Hirota et al., 1985; Noar et al., 1985). Among the various phospholipids tested in vitro, PS is the most effective in activating PKC. Other acidic phos-

† This work was supported by National Institutes of Health Grant GM38737.
* To whom correspondence should be addressed.

[1] Abbreviations: CHAPS, 3-[(3-cholamidopropyl)dimethylammonio]-1-propanesulfonate; DAG, *sn*-1,2-diacylglycerol; HEPES, 4-(2-hydroxyethyl)-1-piperazineethanesulfonic acid; PS, phosphatidylserine; PA, phosphatidate; PP, phosphatidyl-(3-hydroxypropionate); PG, phosphatidylglycerol; PI, phosphatidylinositol; P-Et, phosphatidylethanol; PE, phosphatidylethanolamine; PC, phosphatidylcholine; SM, sphingomyelin.

0006-2960/92/0431-5176$03.00/0